ICES Journal of Marine Science, 60: 1063–1074. 2003
doi:10.1016/S1054–3139(03)00114-0

The influence of ontogeny, physiology, and behaviour on the target strength of walleye pollock (*Theragra chalcogramma*)

John K. Horne

Horne, J. K. 2003. The influence of ontogeny, physiology, and behaviour on the target strength of walleye pollock (*Theragra chalcogramma*). – ICES Journal of Marine Science, 60: 1063–1074.

Variability in echo intensities from aquatic organisms is caused by physical factors associated with the transmission of sound through water, and by biological factors associated with the ontogeny, physiology, and behaviour of targets. Acoustic-based density estimates depend on accurately characterizing reflected or backscattered sound from any species of interest. Digitized lateral and dorsal radiographs of walleye pollock (*Theragra chalcogramma*) were used to characterize intra-specific variability among young-of-the-year, juvenile, and adult life-history stages. Kirchhoff-ray mode (KRM) models were used to quantify variability in backscatter intensities at 38 and 120 kHz. At these geometric scattering frequencies, swimbladder surface areas influence echo intensities. Dorsal swimbladder surface areas were proportionate to fish lengths and decreased after fish were fed. Corresponding changes in backscatter were not proportionate to the reduction in dorsal surface area. The ratio of dorsal to lateral swimbladder surface areas was consistent among gravid and non-gravid fish. Walleye pollock tilt angles were centred at 90° and did not differ among densities or between light and dark cycles. Target strength–length regressions and KRM-predicted backscatter models closely matched *in situ* target-strength measurements for walleye pollock in the Bering Sea. Backscatter variability can be minimized through judicious deployment of equipment and equipment-parameter settings, but the relative influence of biological factors on backscatter amplitude has not been determined.

Keywords: acoustics, behaviour, ontogeny, physiology, target strength, walleye pollock.

Received 2 April 2002; accepted 14 November 2002.

J. K. Horne: University of Washington, School of Aquatic and Fishery Sciences, Box 35520, Seattle, WA 98355, USA; tel: +1 206 221 6890; fax: +1 206 221 6939; e-mail: jhorne@u.washington.edu.

Introduction

Variability in backscattered sound from fish and zooplankton is an accepted attribute of fisheries-acoustic data. This variability cannot be ignored as differences in mean backscattering cross-sections influence density and the resulting abundance or biomass estimates (Forbes and Nakken, 1972; MacLennan and Simmonds, 1992). Early attempts to measure backscattering cross-section, or target strength (TS), used stunned or dead fish (e.g. Midttun and Hoff, 1962; Love, 1971; Nakken and Olsen, 1977), caged animals (e.g. McCartney and Stubbs, 1971; Edwards and Armstrong, 1984; Foote, 1986), or *in situ* measurements (e.g. Ehrenberg, 1979; Foote and Traynor, 1988; Traynor, 1996). Quantifying sources of variability in TSs was not an explicit part of these studies. Renewed interest in developing anatomically based acoustic-backscatter models for fish (e.g. Clay and Horne, 1994; Ye and Furusawa, 1995) and zooplankton (e.g. Martin *et al.*, 1996; Stanton *et al.*, 1996) enables the investigation of biological factors that influence the amount of sound reflected from aquatic organisms.

Biological influences on the amount of sound reflected from aquatic organisms include ontogeny, physiology, and behaviour. From a fisheries-acoustics perspective, the number of variables in each category can be constrained. The definition of ontogeny is restricted to the development and growth of the fish body and swimbladder. Physiology is restricted to fish feeding and gonad development through the reproductive cycle. Behaviour includes the tilt and roll of individual organisms as well as the aggregation (i.e. shoaling) and polarized movement (i.e. schooling) by fish groups.

Walleye pollock (*Theragra chalcogramma*) are used to characterize intra-specific variability in teleost backscattering over a range of life-history stages. Walleye pollock is a commercially harvested species with Bering Sea annual

1054–3139/03/101063+12 $30.00

catches ranging from four to seven million metric tons, representing approximately 5% of the world's fish catch (Bailey *et al.*, 1999). Walleye pollock have been used in previous TS studies for empirical measures (Traynor, 1996) or a combination of backscatter models and measurements (Traynor and Williamson, 1983; Foote and Traynor, 1988; Miyanohana *et al.*, 1990; Sawada *et al.*, 1999). Radiographic "snapshots" of anaesthetized fish are used as input to Kirchhoff-ray mode (KRM) backscatter models (Clay and Horne, 1994) to investigate how acoustic backscatter from walleye pollock is influenced by changes in fish ontogeny, physiology, and behaviour.

Materials and methods

Acoustic-backscatter amplitudes of walleye pollock were estimated using KRM backscatter models. A KRM model uses digitized images of the fish body and swimbladder to estimate total backscatter. Dorsal and lateral radiographs are converted to digital data files by tracing the silhouettes of bodies (not including fins) and swimbladders, scanning the traces, and then electronically digitizing graphic files at 1 mm resolution. Digital files of the fish body and swimbladder are smoothed using a three-point, triangular average. Digitized fish were rotated so that the sagittal axis of the body is aligned with the snout and the tip of the caudal peduncle. The fish body is represented by a set of contiguous fluid-filled cylinders surrounding a set of contiguous gas-filled cylinders used to represent the swimbladder. Backscatter from each cylinder in the body and the swimbladder is estimated and then added coherently to estimate total backscatter as a function of fish caudal length (L in m), dorsal aspect relative to the transducer face (θ in degrees), and acoustic wavelength (λ in m). The acoustic wavelength is a function of the speed of sound in water (c in $m\,s^{-1}$) and the transmitting frequency (f in Hz) (i.e. $\lambda = c/f$). Values for the speed of sound through water, a fish body, and a swimbladder were set at 1470, 1575, and 345 $m\,s^{-1}$. Backscatter amplitudes were calculated for each fish based on the body and swimbladder digital files. Full details of the model can be found in Clay and Horne (1994), Jech *et al.* (1995), or the appendix in Horne and Jech (1999).

Fish used in this study were collected from laboratory tanks at the Hatfield Marine Science Station in Newport, OR. These walleye pollock were raised from eggs fertilized on spawning grounds in the Bering Sea or Shelikoff Strait, Alaska or caught as young-of-the-year fish off the coast of Washington state. Holding tanks for juvenile and adult fish are supplied with ambient seawater and undergo a 12-h light, 12-h dark illumination cycle. A total of 25 juvenile and 20 adult walleye pollock were radiographed (Universal Unimatic 325, model 3487; 84 cm focal length) at dorsal and lateral orientations. Among the juveniles, 10 fish were starved and five fish were fed to repletion prior to being X-rayed. Ten of the adults were starved, five of those fish were fed and re-radiographed. Five other gravid adults were radiographed. Ten additional juvenile fish were radiographed one year later to provide a continuous length range.

Anatomical variation in dorsal and lateral swimbladder surfaces was compared by measuring surface areas using swimbladder digitized files. Dorsal and lateral surface areas were plotted as a function of fish caudal length for juvenile and adult starved and fed fish. The ratio of dorsal to lateral swimbladder surface area was examined as a function of caudal length for starved, fed, and gravid fish. Conversion of caudal length to fork length was determined using linear regression for juvenile, adult, and all fish combined.

To quantify the distribution of walleye pollock tilt orientations, fish were placed in an 8 m^3 tank and aspect angles were measured from still or videotape images. Fish orientation did not appear to be influenced by the size of the tank (but see Tang and Boisclair, 1993). Groups of three or eight fish were placed in the tank and left to acclimate for 8–10 h. A 12-h light and 12-h dark illumination cycle was used throughout the experiments. Low-light infrared cameras were used to image fish orientations during dark hours. Single videoframe images were used to measure tilt angles to the nearest degree with a protractor when the lateral surface of a fish was within 10° of the camera viewplane. A 90° tilt is horizontal. Tilt angles were tabulated for light and dark periods. Mean tilt angles for groups of six replicates were tested for significant differences ($\alpha = 0.05$) between densities and between light and dark replicates.

To quantify the variation in backscatter amplitudes among walleye pollock, the mean and standard deviation backscatter of the 51 modelled fish were predicted as a function of fish length, aspect, and acoustic wavelength. Model estimates were grouped as young-of-the-year (100–250 mm), juveniles (200–400 mm), and adults (350–600 mm). Length groups were purposely overlapped to illustrate the effects of using scaled fish lengths to predict echo amplitudes over specified length ranges. Echo amplitudes were calculated as reduced scattering lengths (RSL), a non-dimensional measure of scattering length (L_{bs} in m) divided by fish length (i.e. $RSL = L_{bs}/L$). RSL values can be converted to the more familiar TS units using $TS = 20\log(RSL) + 20\log(L_{cm})$, where L_{cm} is fish length (fork length for walleye pollock) in centimetres. Concurrence of KRM-model predictions with measured TSs was examined by plotting predicted mean backscatter ± one standard deviation at 90° aspect for 38 and 120 kHz and then superimposing observed *in situ* TS measurements from field surveys in the Bering Sea and Gulf of Alaska (Table 1). KRM-predicted values were also compared to TSs predicted using the empirical regression model from the National Marine Fisheries Service: $TS = 20\log(L_{cm}) - 66$ (Traynor and Williamson, 1983; Foote and Traynor, 1988). All field measurements and model estimates were averaged in the linear domain before being logarithmically transformed to TSs.

Table 1. *In situ* TS measurements of walleye pollock (*T. chalcogramma*) at 38 kHz in the Bering Sea and Gulf of Alaska.

Length (cm)	Target strength (dB)	Sample number	Time	Transducer type	Date	Source
7.7	−46.50	212	Night	Split	9/90	Traynor, 1996
18.0	−41.05	497	Night	Split	2/93	Traynor, 1996
38.0	−33.62	433	Night	Split	3/93	Traynor, 1996
36.3	−35.68	1243	Day	Split	8/94	Traynor, 1996
47.7	−31.67	1555	Day	Dual	6/79	Traynor and Williamson, 1983
46.5	−31.38	1714	Day	Dual	6/79	Traynor and Williamson, 1983
46.5	−32.57	1300	Day	Dual	6/79	Traynor and Williamson, 1983
47.1	−31.82	399	Day	Dual	6/79	Traynor and Williamson, 1983
22.1	−37.59	720	Night	Dual	6/79	Traynor and Williamson, 1983
16.1	−38.34	1343	Night	Dual	6/79	Traynor and Williamson, 1983
41.2	−34.10	1322	Night	Split	8/85	Traynor and Ehrenberg, 1990
42.4	−33.0	363	Night	Split	8/85	Traynor and Ehrenberg, 1990

The ability to incorporate fish-tilt variation in predicted TSs was investigated by comparing *in situ* TS distributions to KRM-predicted TSs. A portion of an acoustic transect surveyed at 38 and 120 kHz on July 19, 2000 on the Bering Sea Shelf was used to compile walleye pollock *in situ* TSs. Corresponding length–frequency distributions were compiled from two mid-water trawl samples taken at a single location (55°55.2′N, 173°27.0′W) chosen for its low overall target density and the dominance (>98%) of pollock in trawl catches. KRM-predicted TS distributions were computed using a representative walleye pollock (number 17, CL = 390 mm), the length–frequency distribution from haul 77 (n = 427), and the tank-tilt frequency distribution. For a specified number of fish, TSs were calculated based on randomly chosen lengths and tilts from the appropriate frequency distributions. The probability of choosing any length or tilt was weighted by the frequency of occurrence.

Results

Ontogeny

The caudal length of walleye pollock was linearly proportional to fork length in the three life-history stages (Figure 1a–c) and when all fish were grouped (Figure 1d).

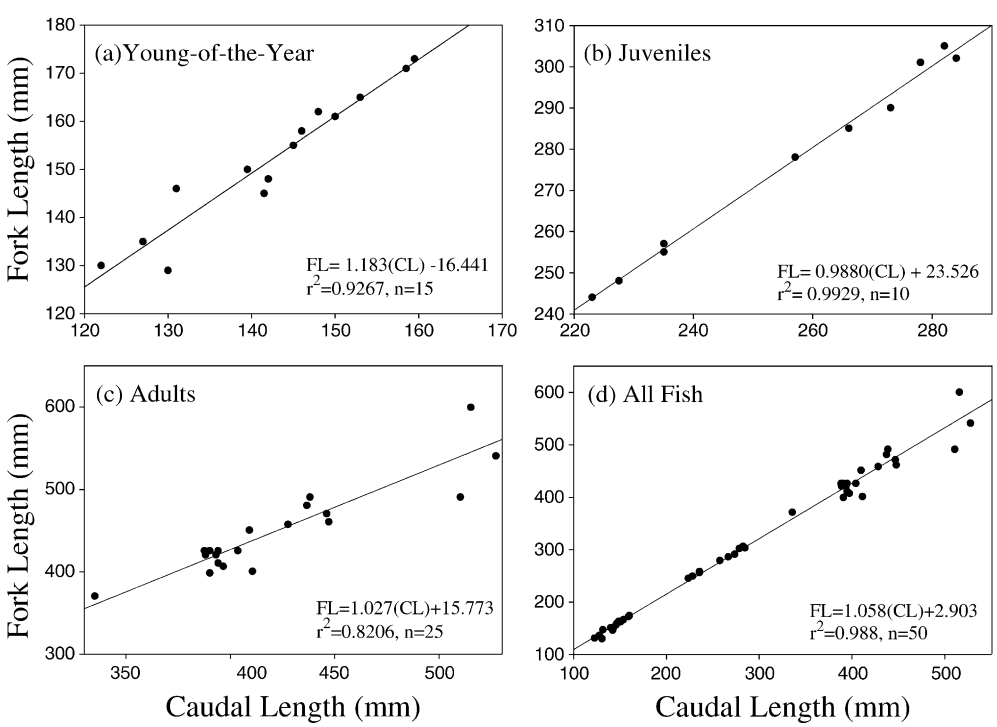

Figure 1. Fork length (FL in mm) plotted as a function of caudal length (CL in mm) for (a) young-of-the-year (n = 15), (b) juvenile (n = 10), (c) adult (n = 25), and (d) all walleye pollock (n = 50) combined.

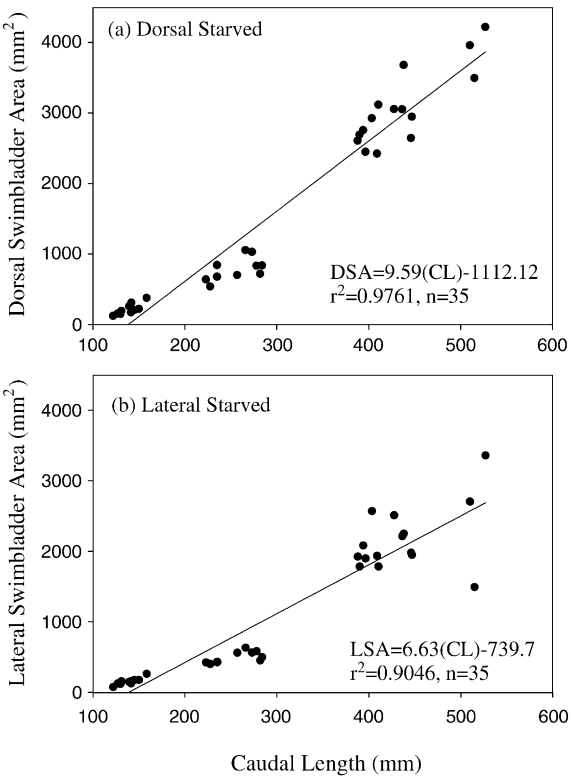

Figure 2. (a) Dorsal and (b) lateral walleye pollock (n = 35) swimbladder surface area (mm^2) plotted as a function of caudal length (mm). Only starved fish were used in these plots to avoid changes in swimbladder shape due to peritoneal contents.

Dorsal swimbladder surface areas (DSA) increased with caudal length (Figure 2a) and were consistently larger than lateral swimbladder surface areas (LSA) (Figure 2b) among young-of-the-year, juvenile, and adult walleye pollock. Juvenile swimbladder surface areas were consistently below that predicted by both dorsal and lateral linear regressions. The 15 radiographs of fed and gravid fish were excluded from the sample to prevent distortion of swimbladder shape due to gut cavity contents.

Physiology

The feeding cycle potentially introduces variability in swimbladder surface areas. As observed among starved fish, DSA (Figure 3a) were larger than LSA (Figure 3b) among 11 fed walleye pollock. Variability in swimbladder areas among starved (Figure 2a, b) and fed (Figure 3a, b) adult fish exceeded that observed among young-of-the-year walleye pollock. To examine the direct effect of feeding on DSA, five adult pollock were radiographed with empty stomachs and then after being fed to repletion. DSA decreased after fish were fed in every case (Figure 3c). The decrease ranged from a minimum of 68.3 mm^2 in the smallest fish to a maximum of 515.8 mm^2 in a 407 mm fish.

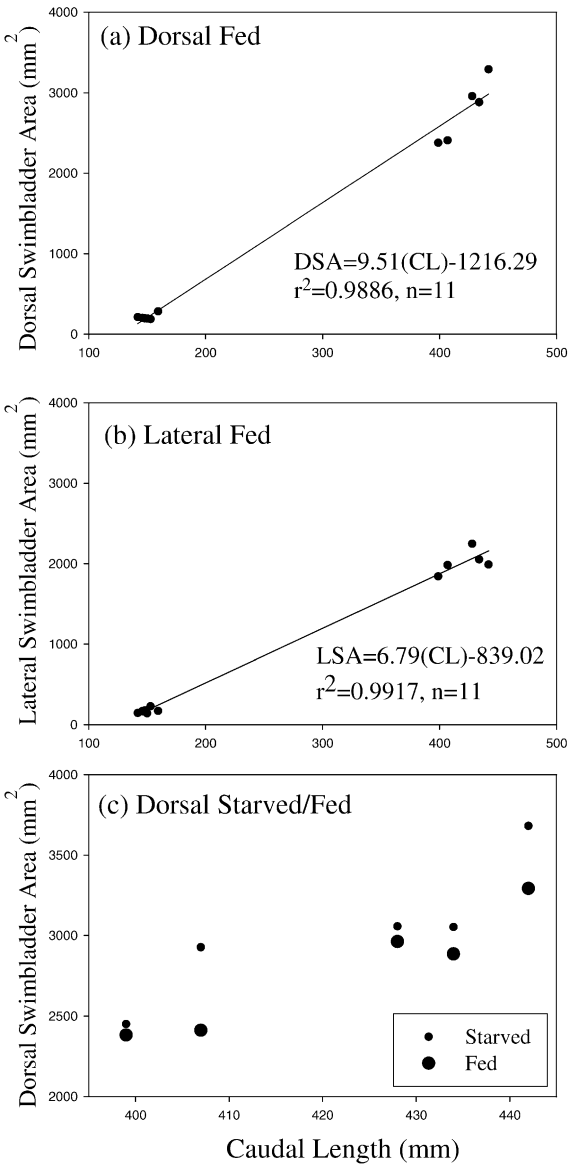

Figure 3. (a) Dorsal and (b) lateral swimbladder surface areas (mm^2) of fed walleye pollock (n = 11) plotted as a function of caudal length (mm). (c) dorsal swimbladder areas of starved (small dots) and then fed (large dots) adult walleye pollock plotted as a function of caudal length (mm). Dorsal surface areas decreased in all cases after the fish were fed.

Any change in dorsal surface area of the swimbladder will influence the amount of sound reflected by a fish.

The effect of gonad production on swimbladder area was investigated by comparing the ratio of dorsal to lateral surface area as a function of fish length between non-gravid and gravid fish that had not been fed (Figure 4). All starved, non-gravid fish were plotted to illustrate potential length- or age-dependent influences on the metric. Dorsal swimbladder

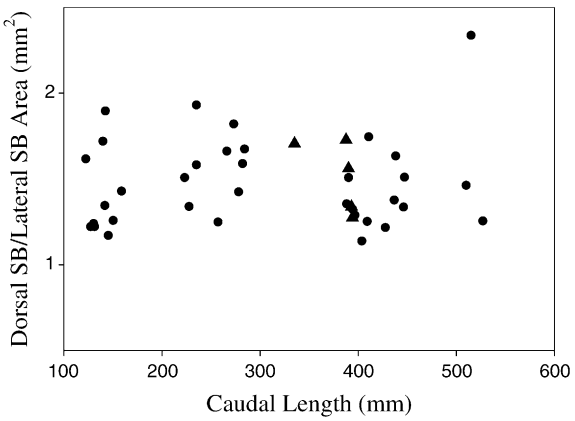

Figure 4. Ratio of dorsal to lateral swimbladder (SB) surface area (mm^2) of starved (circles) and gravid walleye pollock (triangles) plotted as a function of caudal length (mm).

areas exceeded lateral swimbladder areas in every case (i.e. all values of the ratio were greater than 1). Among starved fish, the ratio of dorsal to lateral swimbladder area averaged 1.48 and ranged from a minimum of 1.14 to a maximum of 2.34. Ratio values of the five gravid fish did not exceed values of other similar sized fish.

Behaviour

There were no significant differences in tilt angle distributions from observations of walleye pollock in the 8 m^3 tank among replicates of dark and light cycles ($n = 6$, $p = 0.886$, $df = 1$) or among high- and low-density fish groups ($n = 6$, $p = 0.170$, $df = 1$). Because tilt distributions did not differ among treatments, all tilt data were combined. The resulting tilt frequency distribution was leptokurtic with tilt angles ranging from 0° to 180° (Figure 5). The large modal tilt at 90° indicates that fish were typically maintaining a horizontal aspect within the tank. Extreme angles indicate that fish were moving between the surface and the bottom of the tank or were oriented to a tank wall. Roll angles were not easily measured from photographic or video "snapshots" of individual fish orientations. Visual inspection of the pictures indicated that roll angles of fish did not appear to deviate from the vertical plane (E. Sturm, Hatfield Marine Science Center, personal communication).

Comparing backscatter-model predictions to measures

Backscatter models can be used to examine the effect of changing swimbladder areas on predicted TSs. Differences in TSs at 38 and 120 kHz (Figure 6) were estimated using KRM backscatter models for the five starved and fed adult pollock (cf. Figure 3c). At 38 kHz predicted TSs of starved fish were greater in four of five cases. The difference in TS was not proportional to the difference between dorsal and lateral swimbladder areas. Clear patterns in TS differences were not evident at 120 kHz. Predicted TSs for three of the five starved fish were lower (up to 9 dB) than TSs of the fed fish. No consistent pattern in TS change with change in dorsal swimbladder surface area existed at 120 kHz. The small sample size precludes any definitive conclusions on the dependence of TS on swimbladder area but the results

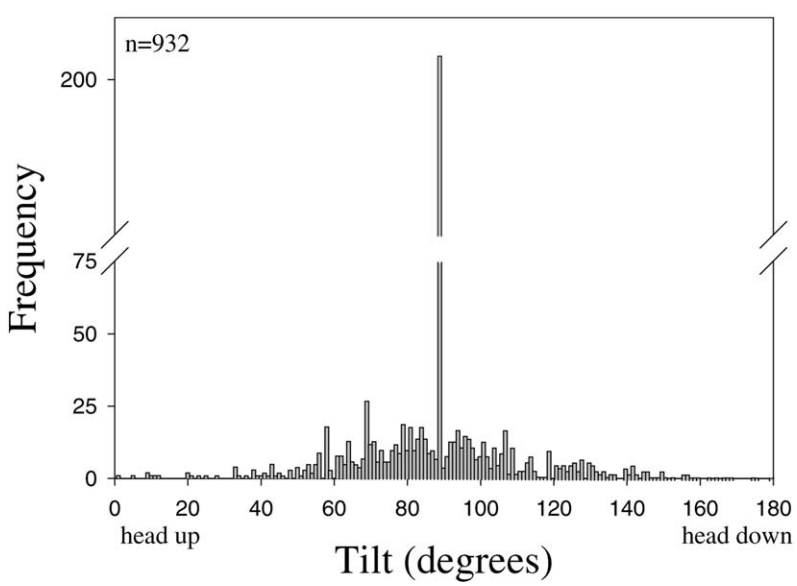

Figure 5. Frequency distribution of walleye pollock tilts ($n = 932$) observed in an 8 m^3 tank. Horizontal aspect is 90°, less than 90° is head-up, greater than 90° is head-down. No differences in tilt distributions were observed during light hours compared to dark hours, or at low ($n = 3$) compared to high ($n = 8$) densities.

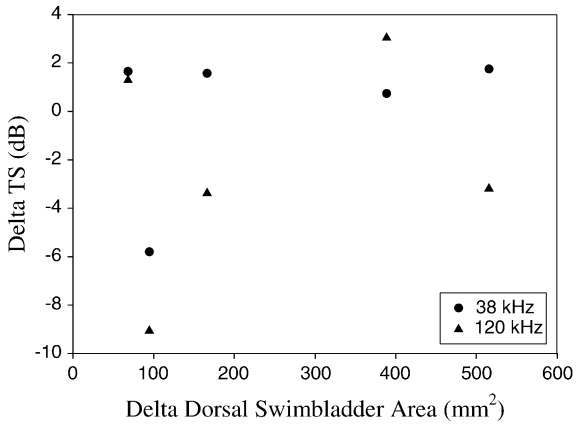

Figure 6. Change in TS (ΔTS in dB) of five walleye pollock at 38 kHz (circles) and 120 kHz (triangles) plotted as a function of the change in dorsal swimbladder surface area (starved − fed fish in mm^2).

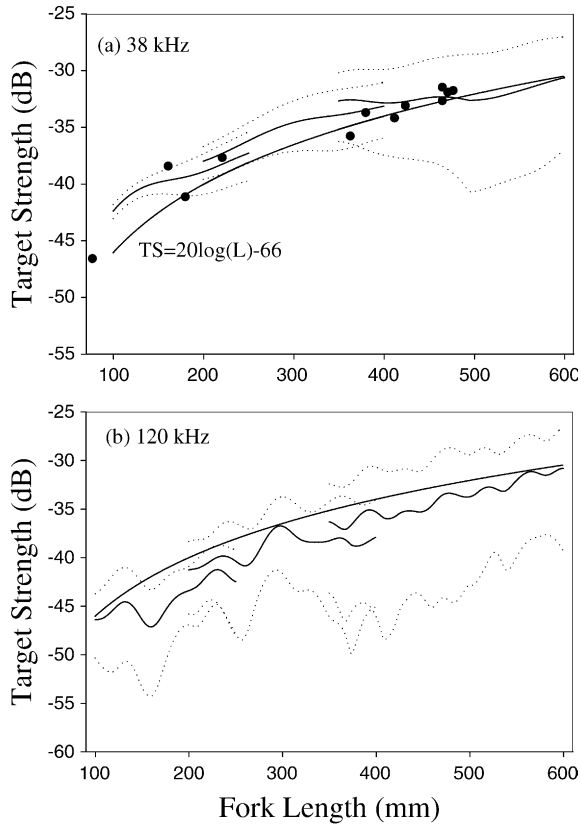

Figure 7. Target strength (dB) plotted as a function of walleye pollock fork length (mm) at (a) 38 kHz and (b) 120 kHz. In each plot the segmented line is the mean KRM-predicted TS, the dotted line is one standard deviation from the KRM mean, the solid line is the 38 kHz TS–length regression model used by NMFS Alaska Fisheries Science Center. The solid points are mean *in situ* TSs and length catches from Bering Sea samples (cf. Table 1).

illustrate the complex relationship between swimbladder surface area and TS.

KRM backscatter models from all radiographed fish (n = 50) were used to compile TS–length curves at 38 and 120 kHz (Figure 7). Each curve comprised three overlapping length sections based on young-of-the-year, juvenile, and adult life-history stages (see Figure 1 for numbers and lengths of fish). This approach prevents excessive scaling of individual fish lengths when estimating TS over a specified length range. For comparison, mean *in situ* TSs were overlaid on the same plot. All but one of the 38 kHz *in situ* average TS values (Table 1) fall within one standard deviation of the KRM-predicted TS curve. Empirical TS values from adult fish are closer to KRM predictions than values from smaller fish. Values predicted from the TS–length regression and the KRM models are in close agreement with empirical points at fish lengths greater than 380 mm. The regression curve lies below the KRM curve at fish lengths below 490 mm. The greatest disparity among the three data sources occurs at fish lengths below 200 mm suggesting that additional modelling and measuring of juvenile and young-of-the-year walleye pollock TS is warranted.

One application of backscatter modelling incorporates behaviour in predictions of TS. An *in situ* TS (38 and 120 kHz) and two length–frequency distributions from the Bering Sea were used as representative adult walleye pollock size distributions (Figure 8). Fish-length samples from both trawl hauls were unimodal and differed by less than 1 cm in mean length (41.3 cm haul 77; 42.0 cm haul 78). *In situ* TSs were filtered to match the depth range of the net opening (80–100 m) and to occur within 3 dB of acoustic axes. A TS threshold of −65 dB was used during *in situ* collections for both frequencies. The 38 kHz TS frequency distribution had three TS clusters with modal peaks occurring at approximately −57, −38 and −27 dB (Figure 8c). The 120 kHz TS frequency distribution was closer to a normal distribution with a strong mode at −35 dB and smaller peaks at −54 and −64 dB (Figure 8d). Simulations of TS frequency distributions (Figure 9) using the KRM model, length frequencies from trawl haul 77 (Figure 8a), and the tank-tilt frequency distribution (Figure 5) produced similar results to the *in situ* walleye pollock TS distributions. At 38 kHz, the three independently simulated TS frequency distributions (Figure 9a–c) had modes corresponding to *in situ* TS modes at approximately −27 and −34 dB. A third grouping of TSs centred at approximately −55 dB indicated a presence of smaller target returns but was not proportionate to that recorded *in situ* (Figure 8c). Similar correspondence was observed at 120 kHz. Predicted TS distributions (Figure 9d–f) were essentially unimodal with a dominant peak at −38 dB and a left tail extending down to −70 dB. Small peaks were visible at −54 dB and at

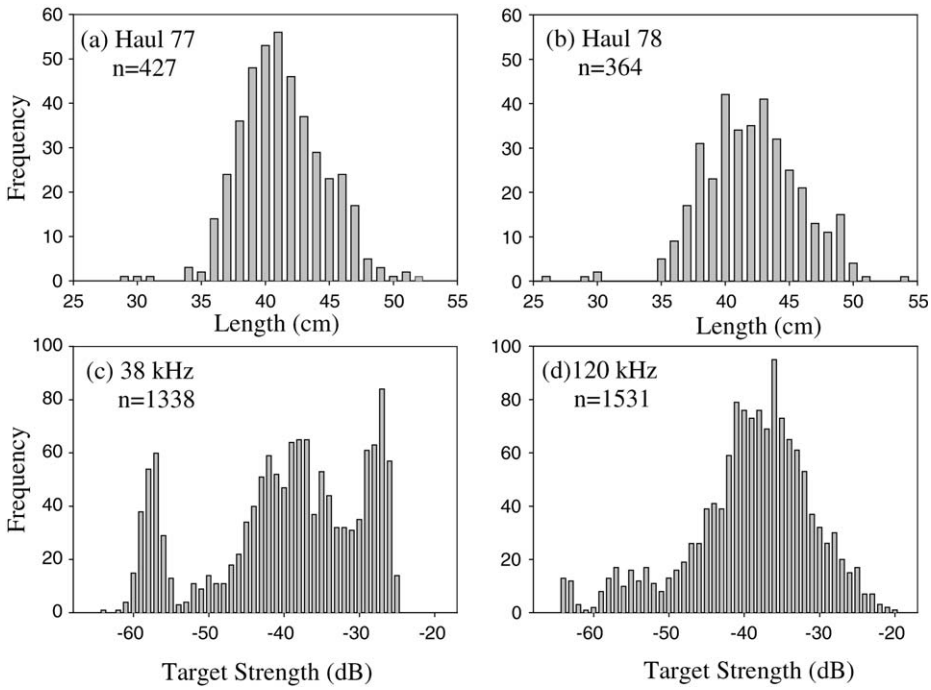

Figure 8. Walleye pollock length–frequency distributions (cm) from (a) haul 77 and (b) haul 78 from the same location in the Bering Sea on July 19, 2000. Frequency distributions of *in situ* walleye pollock TSs (dB) at (c) 38 kHz and (d) 120 kHz sampled between hauls 77 and 78.

approximately −60 dB. Skewed left tails in simulated TS distributions at 38 and 120 kHz suggest that *in situ* data collections should not be truncated at −65 dB (Figure 8c, d). KRM-simulated TS frequency distributions did not replicate those compiled from *in situ* measurements but did match dominant TS modes and the overall shape of TS frequency distributions.

Discussion

Characteristics of sound transmission through water are well documented (e.g. Medwin and Clay, 1997), but the understanding of backscattered sound from dynamic, aquatic organisms is not complete. This study illustrates that ontogeny, physiology, and behaviour potentially influence the magnitude and range of backscattered sound within a single species. Anatomical differences among species increases the potential for backscatter variability of *in situ* TS measurements in mixed aggregations of fish.

Ontogenetic changes in fish length and swimbladder proportions will affect the amount of sound reflected by an individual fish. Changes in backscatter amplitude from individual fish are not tracked over time but any non-linear growth will influence TS to fish-length regressions used to convert acoustic size to fish length. Allometric changes in swimbladder volume have been documented for teleost species (e.g. Butler and Pearcy, 1972) and among individuals (e.g. Gee, 1968) but TS–length regressions are not typically restricted to specified length ranges. A single TS–length regression may not be appropriate for all life-history stages (cf. Figure 7). In this study DSA were proportionate to walleye pollock lengths, but there was no linear relationship between swimbladder surface area and TS. The standard practice of restricting *in situ* TS collections to occasions when single fish species are present in unimodal length groups will minimize ontogenetic effects on backscatter.

Food in the stomach and gonad production alters the volume and shape of a gas-filled swimbladder. Ona (1990) found that stomach contents of Atlantic cod (*Gadus morhua*) reduced swimbladder volumes by up to 90% and gonad presence reduced mean swimbladder volume by as much as 35%. Most swimbladder volume reduction occurs in the dorso-ventral plane (Arnold and Greer Walker, 1992), with one (e.g. Atlantic cod, Ona, 1990) or both (e.g. Atlantic herring, Blaxter *et al.*, 1979) ends of the bladder collapsing before the middle section. Reductions in swimbladder length and volume will influence swimbladder areas. The presence of food in walleye pollock stomachs reduced walleye pollock dorsal swimbladder areas by 2.8–17.6%. Ratios of dorsal to lateral swimbladder area among gravid walleye pollock did not differ from non-gravid fish, but ovaries and testes were not fully developed at the time of sampling.

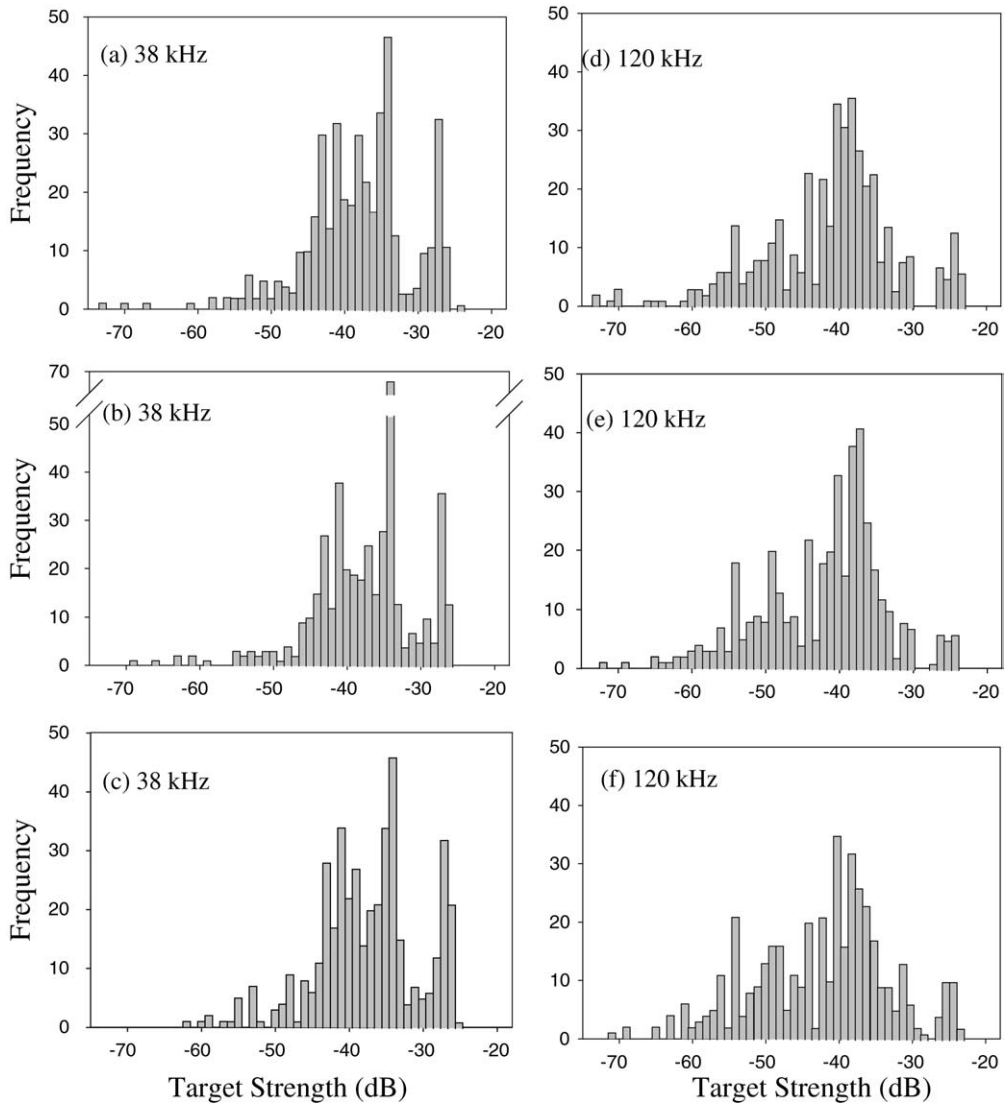

Figure 9. Walleye pollock simulated TS frequency distributions at 38 kHz (a–c) and 120 kHz (d–f) using KRM backscatter model predictions from the length frequencies in haul 77 (cf. Figure 8a) and the aspect frequency distribution from tank observations (cf. Figure 3). The probability of any fish length or tilt angle used in KRM calculations is weighted by the frequency of occurrence.

From a fish's perspective, depth and aspect are the two behavioural factors influencing backscatter that are under direct control. Since an air-filled swimbladder is responsible for at least 90% of backscattered sound (Foote, 1980a), pressure-induced changes in swimbladder volume (Boyle's law: at constant temperature, volume $\propto$ pressure^{-1}) and subsequent changes in swimbladder surface areas will affect TS. Maximum TSs of kokanee salmon (*Oncorhynchus nerka*) decreased by 10 dB when lowered from 5 to 40 m depth (Mukai and Iida, 1996). Experiments using Atlantic cod found that swimbladder volumes conformed to Boyle's law over pressure increases of up to 10 atm, but changes in swimbladder surface areas were not proportional to pressure increases (Ona, 1990). Since the dorsal swimbladder surface is constrained by the spinal column and pleural ribs, the swimbladder is not expected to act like a free bubble. Pictures of partially dissected herring (*Clupea harengus*) under pressure showed that swimbladders compressed dorso-laterally into shallow ellipses (cf. Figure 2, Blaxter *et al.*, 1979). At 3.25 atm, ventral-surface swimbladder areas were reduced by an average of 43% relative to the surface area at 1 atm. The effects of depth on swimbladder volume and surface areas have not been quantified for walleye pollock.

Fish tilt is often used to compensate for lost buoyancy when swimming at depth. The aspect of an individual fish relative to the incident acoustic wave front has a large potential impact on echo intensity. At a 30° angle from

horizontal, Foote (1980b) reports a 30 dB reduction in TS of Atlantic cod relative to the maximum TS measured. Teleost swimbladders are typically angled posterior-down relative to the medial axis of the fish (cf. Blaxter and Batty, 1990; Clay and Horne, 1994). Empirical measurements and theoretical calculations show that maximum backscatter will occur when the swimbladder surface closest to the sound source is orthogonal to the incident-wave front (Foote, 1980b). Sensitivity of TS to tilt angle increases with an increase in the ratio of fish length to acoustic wavelength (Johannesson and Mitson, 1983; Horne, 2000). Recognizing the importance of fish aspect, Olsen (1977) and Foote (1980c) developed TS–length regression models that incorporate fish-aspect distributions and transducer-beam shapes to predict mean backscatter amplitudes for Atlantic cod. This practice is not routine when converting acoustic sizes to fish lengths for fish-density or population-abundance estimates.

The single, dominant peak at 90° (i.e. horizontal) in the frequency histogram of fish aspects from tank observations (Figure 5) is refreshing news for *in situ* TS collections of walleye pollock. Even if swimbladder angles within fish differ from horizontal, the negative bias in TS frequency distributions should be relatively constant. Additional observations of uniform size (Ranta and Lindström, 1990; Ranta *et al.*, 1992) and behaviour (Partridge *et al.*, 1980; Aoki, 1984) among fish within aggregations will also reduce variability in backscatter amplitudes from individual targets. *In situ* tilt frequency distributions of walleye pollock have not been reported.

Backscatter amplitudes from regression analyses and *in situ* average TS measures differed from those predicted using KRM backscatter models. These values did not typically differ by more than 3 dB at 38 or 120 kHz. At 38 kHz, predicted TSs from the regression model were consistently less than those predicted using the KRM numeric model for fish less than 500 mm. Differences between empirical and numeric models generally increased as fish length decreased. Very few *in situ* walleye pollock TS measurements less than 380 mm are available for comparison (cf. Traynor, 1996). KRM-predicted TSs exceeded those predicted by the $20\log(L)-66$ regression equation over the entire modelled length range at 120 kHz. The fact that the two 120 kHz results differ is not surprising since 38 kHz data were used to develop the TS–length regression model and a frequency term was not included in the regression to compensate for frequency-dependent backscatter (*sensu* Love, 1971, 1977). Observed differences between model predictions and measurements of walleye pollock TS are not unique. Sawada *et al.* (1999) showed that at aspect angles of 90°, 38 kHz predicted TSs from deformed-cylinder (Ye, 1997; Ye *et al.*, 1997) and prolate-spheroid (Furusawa, 1988) backscatter models differed by as much as 13.5 dB from measurements of four dead walleye pollock in a freshwater tank. Traynor (1996) superimposed estimated TS distributions derived using length–frequency distributions from trawl samples and a TS–length regression model on *in situ* TS distributions. Modal peaks of the regression-based TS frequency distributions were close to modal peaks of the *in situ* TS distributions, but the general shapes of trawl-based TS frequency distributions matched trawl length–frequency distributions better than shapes of the *in situ* TS distributions.

Few studies use numeric backscatter models to derive TS–length relationships. In this study all walleye pollock predicted TSs were based on radiographs of live, anaesthetized fish. Backscatter amplitudes were predicted for each fish over specified length, frequency, or tilt-angle ranges. In an earlier study, Foote and Traynor (1988) used the interpolation of sectioned swimbladders, theoretical tilt-angle distributions, and a finite-element realization model (cf. Foote, 1985) to estimate probability distributions of walleye pollock TSs. In contrast, freshly killed (Miyanohana *et al.*, 1990) or frozen (Sawada *et al.*, 1999) fish have been used when measuring TSs of tethered walleye pollock. Dead fish are not appropriate for TS measurements. Post-mortem loss of muscle tone influences the amount of sound reflected by fish (Clark *et al.*, 1975). Swimbladder-resonance frequencies have been shown to drop within 15 minutes of mortality (Cox and Rogers, 1987) and an associated change in geometric backscatter is expected. The alternate approach of comparing carefully filtered, *in situ*, TS measurements to trawl-catch lengths (e.g. Traynor, 1996) assumes that *in situ* TS measurements are from single targets and that trawl samples provide representative length–frequency distributions. No current method provides definitive TS–length measurements in natural conditions.

Despite basing population TSs on modelled backscatter from a single fish, KRM predictions mimicked empirical TS frequency distributions at both frequencies. Evaluating results relative to both techniques provides insight into the detection and conversion of single acoustic targets to fish lengths. The presence of TSs above −30 dB in empirical TS frequency distributions suggests that large fish were present during *in situ* measurements and were not caught in the trawl, that single TS measurements exceeded those predicted by the TS–length equation, or that multiple targets were accepted by the echo sounder. Fish lengths did not exceed 55 cm in either of the trawl hauls but the Aleutian wing trawl used in this study has caught fish larger than 55 cm and smaller than 25 cm at other times and locations (J. Horne, personal observation). The walleye pollock TS–length regression equation predicts that a −30 dB target would correspond to a 63 cm fish. TS to length regression equations reflect average TSs measured from low density, unimodal fish aggregations. Modelling and empirical experiments have shown that maximum TSs are reflected from individual fish at slightly-head-down aspects.

Splitbeam echosounders are known to accept multiple echoes as single targets (Soule *et al.*, 1995; Barrange *et al.*, 1996; Soule *et al.*, 1996), but the probability of multiple echoes at the location and depths sampled only ranged from

3.2 to 14.8% (cf. Ona, 1999). Splitbeam echosounders may also bias TS measurements to smaller targets (Foote, 1996; Ona and Barrange, 1999). The depth range sampled and sizes of fish caught suggest that TS measurements should not be biased toward small walleye pollock (cf. Traynor, 1996). The KRM-modelling exercise also demonstrated that very large and very small TSs are possible even with a narrow length–frequency distribution and a tilt distribution heavily weighted at 90°. Small predicted TSs (≤ -60 dB) could result from small lengths combined with large aspect angles.

Another potential cause of low TSs and bimodal TS distributions in empirical TS frequency distributions is non-point source backscatter by fish. Examples of bimodal TS frequency distributions associated with unimodal length–frequency distributions from net catches include walleye pollock (Figure 3, Williamson and Traynor, 1984), Atlantic cod (Figure 2, Clay and Castonguay, 1996; Figure 4, Hammond, 1997) and hoki (*Macruronus novaezelandiae*) (Figure 1, Cordue *et al.*, 2001). The most striking example is Traynor's (1996) Figure 1 where the TS frequency-distribution bimodality increases with fish length. Many authors state the potential for contamination by other species and the bias against small targets as possible causes, but contamination or bias are not expected to obscure modal peaks in TS frequency distributions. Quasi-periodic shifts in TS of tracked or tethered fish (e.g. Dawson and Karp, 1990; Horne *et al.*, 2000) suggest that swimming motion may influence backscatter amplitudes (although see Foote, 1985) and contribute to bimodal TS frequency distributions. The direct effect of swimming on TS variability has not been documented or explained.

Current acoustic-survey practices are designed to minimize TS variability. Regulating survey times minimizes the influence of ontogeny and physiology. Annual surveys conducted at the same time each year will minimize the range of potential TSs due to rapid growth of young-of-the-year fish. Surveys on post-spawning fish reduce the contributions to backscatter variability from food or gonad in the peritoneal cavity. Zhao (1996) found that TSs of gravid herring increased by approximately 2 dB compared to fish in spent or resting reproductive stages. To directly address variable survey times, Ona *et al.* (2000) proposed using a herring TS equation that explicitly includes a gonadosomatic index (i.e. GSI) term. Behavioural effects are minimized through equipment deployment and parameter settings. Surveys restricted to light or dark hours minimize changes in fish-aspect angles, depth changes, and fish densities. Surveying pelagic fish during dark hours also maximizes the probability of measuring individual TSs when fish are dispersed (Brandt *et al.*, 1991). The sensitivity of TS to fish aspect is minimized by an acoustic frequency that minimizes the fish-length to acoustic-wavelength ratio (cf. Horne and Clay, 1998). A short pulse duration coupled with a short acoustic wavelength increases target resolution within the acoustic beam but potentially increases backscatter variability because of sensitivity to fish orientation.

Variability in backscatter amplitudes due to biological sources is not traditionally partitioned within acoustic measurements. Quantifying the relative importance of biological and physical factors that influence backscatter amplitudes will identify variables that should be included when converting acoustic sizes to fish lengths, and potential research areas that will enhance the understanding of sound scattering by aquatic organisms.

Acknowledgements

The Staff of the Alaska Fisheries Science Center, Behavioral Group at the Hatfield Marine Science Center are thanked for supplying fish and assisting with radiographs. The Pine Grove Veterinary Clinic provided access to radiographic and developing equipment. Michael Davis conducted the fish-tilt trials with measurements by Erik Sturm and Mora Spencer. Neal Williamson supplied walleye pollock length–frequency and *in situ* TS data. Elliott Hazen assisted with the juvenile pollock radiographs, digitizing data, and running KRM models. The manuscript benefited from comments by Stéphane Gauthier, Paul Walline, Neal Williamson, and an anonymous reviewer. This work was supported by the NOAA NMFS Alaska Fisheries Science Center and a grant from the Office of Naval Research (N00014-00-1-0180).

References

Aoki, I. 1984. Internal dynamics of fish schools in relation to inter-fish distance. Bulletin of the Japanese Society of Scientific Fisheries, 50: 751–758.

Arnold, G. P., and Greer Walker, M. 1992. Vertical movements of cod (*Gadus morhua* L.) in the open sea and the hydrostatic function of the swimbladder. ICES Journal of Marine Science, 49: 357–372.

Bailey, K. M., Quinn, T. J., II, Bentzen, P., and Grant, W. S. 1999. Population structure and dynamics of walleye pollock, *Theragra chalcogramma*. Advances in Marine Biology, 37: 179–255.

Barrange, M., Hampton, I., and Soule, M. 1996. Empirical determination of *in situ* target strengths of three loosely aggregated pelagic fish species. ICES Journal of Marine Science, 53: 225–232.

Blaxter, J. H. S., and Batty, R. S. 1990. Swimbladder "behavior" and target strength. Rapports et Process-Verbaux des Reunions Commission Internationale pour Exploration de la Mer, 189: 233–244.

Blaxter, J. H. S., Denton, E. J., and Gray, J. A. B. 1979. The herring swimbladder as a gas reservoir for the acoustico-lateralis system. Journal of the Marine Biological Association of the United Kingdom, 59: 1–10.

Brandt, S. B., Mason, D. M., Patrick, E. V., Argyle, R. L., Wells, L., Unger, P. A., and Stewart, D. J. 1991. Acoustic measures of the abundance and size of pelagic planktivores in Lake Michigan. Canadian Journal of Fisheries and Aquatic Sciences, 48: 894–908.

Butler, J. L., and Pearcy, W. G. 1972. Swimbladder morphology and specific gravity of myctophids off Oregon. Journal of the Fisheries Research Board of Canada, 29: 1145–1150.

Clark, N. L., Popper, A. N., and Mann, J. A., Jr. 1975. Laser light-scattering investigations of the teleost swimbladder response to acoustic stimuli. Biophysical Journal, 15: 307–318.

Clay, A., and Castonguay, M. 1996. *in situ* target strengths of Atlantic cod (*Gadus morhua*) and Atlantic mackerel (*Scomber scombrus*) in the Northwest Atlantic. Canadian Journal of Fisheries and Aquatic Sciences, 53: 87–98.

Clay, C. S., and Horne, J. K. 1994. Acoustic models of fish: the Atlantic cod (*Gadus morhua*). Journal of the Acoustical Society of America, 96: 1661–1668.

Cordue, P. L., Coombs, R. F., and Macaulay, G. J. 2001. A least-squares method of estimating length to target-strength relationships from *in situ* target-strength distributions and length frequencies. Journal of the Acoustical Society of America, 109: 155–163.

Cox, M., and Rogers, P. H. 1987. Automated non-invasive motion measurement of auditory organs in fish using ultrasound. Journal of Vibration, Stress, and Reliability in Design, 109: 55–59.

Dawson, J. J., and Karp, W. A. 1990. *in situ* measures of target-strength variability of individual fish. Rapports et Process-Verbaux des Reunions Commission Internationale pour Exploration de la Mer, 189: 264–273.

Edwards, J. I., and Armstrong, F. 1984. Target-strength experiments on caged fish. Scottish Fisheries Bulletin, 48: 12–20.

Ehrenberg, J. E. 1979. A comparative analysis of *in situ* methods for directly measuring the acoustic target strength of individual fish. IEEE Journal of Ocean Engineering, OE-4: 141–152.

Foote, K. G. 1980a. Importance of the swimbladder in acoustic-scattering fish: a comparison of gadoid and mackerel target strengths. Journal of the Acoustical Society of America, 67: 2064–2089.

Foote, K. G. 1980b. Effect of fish behaviour on echo energy: the need for measurements of orientation distributions. Journal du Conseil International pour l'Exploration de la Mer, 39: 193–201.

Foote, K. G. 1980c. Averaging of fish target-strength functions. Journal of the Acoustical Society of America, 67: 504–515.

Foote, K. G. 1985. Effect of swimming on fish target strength. ICES CM 1985/B: 29. 6 pp.

Foote, K. G. 1986. A critique of Goddard and Welsby's paper "The acoustic target strength of live fish". Journal du Conseil International pour l'Exploration de la Mer, 42: 212–220.

Foote, K. G. 1996. Coincidence echo statistics. Journal of the Acoustical Society of America, 99: 266–271.

Foote, K. G., and Traynor, J. J. 1988. Comparison of walleye pollock target-strength estimates determined from *in situ* measurements and calculations based on swimbladder form. Journal of the Acoustical Society of America, 83: 9–17.

Forbes, S. T., and Nakken, O. eds. 1972. Manual of methods for fisheries-resource survey and appraisal. Part 2. The use of acoustic instruments for fish detection and abundance estimation. FAO Manuals in Fisheries Science, 5: 1–138.

Furusawa, M. 1988. Prolate-spheroidal models for predicting general trends of fish target strength. Journal of the Acoustical Society of Japan, 9: 13–24.

Gee, J. H. 1968. Adjustment of buoyancy by longnose dace (*Rhinichthys cataractae*) in relation to velocity of water. Journal of the Fisheries Research Board of Canada, 25: 1485–1496.

Hammond, T. 1997. A Bayesian interpretation of target-strength data from the Grand Banks. Canadian Journal of Fisheries and Aquatic Sciences, 54: 2323–2333.

Horne, J. K. 2000. Acoustic approaches to remote species identification: a review. Fisheries Oceanography, 9: 356–371.

Horne, J. K., and Clay, C. S. 1998. Sonar systems and aquatic organisms: matching equipment and model parameters. Canadian Journal of Fisheries and Aquatic Sciences, 55: 1296–1306.

Horne, J. K., and Jech, J. M. 1999. Multi-frequency estimates of fish abundance: constraints of rather-high frequencies. ICES Journal of Marine Science, 56: 184–199.

Horne, J. K., Walline, P. D., and Jech, J. M. 2000. Comparing acoustic model predictions to *in situ* backscatter measurements of fish with dual-chambered swimbladders. Journal of Fish Biology, 57: 1105–1121.

Jech, J. M., Schael, D. M., and Clay, C. S. 1995. Application of three sound-scattering models to threadfin shad (*Dorosoma petenense*). Journal of the Acoustical Society of America, 98: 2262–2269.

Johannesson, K. A., and Mitson, R. A. 1983. Fisheries acoustics. FAO Fisheries Technical Paper, 249 pp.

Love, R. H. 1971. Dorsal-aspect target strength of an individual fish. Journal of the Acoustical Society of America, 49: 816–823.

Love, R. H. 1977. Target strength of an individual fish at any aspect. Journal of the Acoustical Society of America, 62: 1397–1403.

MacLennan, D. N., and Simmonds, E. J. 1992. Fisheries Acoustics. Chapman and Hall, London. 325 pp.

Martin, L. V., Stanton, T. K., Wiebe, P. H., and Lynch, J. F. 1996. Acoustic classification of zooplankton. ICES Journal of Marine Science, 53: 217–224.

McCartney, B. S., and Stubbs, A. R. 1971. Measurements of the acoustic target strengths of fish in dorsal aspect, including swimbladder resonance. Journal of Sound Vibration, 15: 397–420.

Medwin, H., and Clay, C. S. 1997. Applied Ocean Acoustics: Fundamentals of Acoustical Oceanography. Academic Press, New York. 712 pp.

Midttun, L., and Hoff, I. 1962. Measurements of the reflection of sound by fish. FiskeriDirectoratets Skrifter Serie HavUndersokelser, 13: 1–18.

Miyanohana, Y., Ishii, K., and Furusawa, M. 1990. Measurements and analyses of dorsal-aspect target strength of six species of fish at four frequencies. Rapports et Procés-Verbaux des Réunions du Conseil International pour l'Exploration de la Mer, 189: 317–324.

Mukai, T., and Iida, K. 1996. Depth dependence of target strength of live kokanee salmon in accordance with Boyle's law. ICES Journal of Marine Science, 53: 245–248.

Nakken, O., and Olsen, K. 1977. Target-strength measurements of fish. Rapports et Procés-Verbaux des Réunions du Conseil International pour l'Exploration de la Mer, 170: 53–69.

Olsen, K. 1977. Orientation measurements of the cod in Lofoten obtained from underwater photographs and their relation to target strength. ICES CM 1977/B: 25. 1–8.

Ona, E. 1990. Physiological factors causing natural variations in acoustic target strength of fish. Journal of the Marine Biological Association of the United Kingdom, 70: 107–127.

Ona, E. (Ed.) 1999. Methodology for target-strength measurements. ICES Cooperative Research Report, 235. 59 pp.

Ona, E., and Barrange, M. 1999. Single target recognition. ICES Cooperative Research Report, 235: 28–43.

Ona, E., Zhao, X., Svellingen, I., and Fosseidengen, J. E. 2000. Seasonal variations in herring target strength. *In* Proceedings of the Herring 2000: Expectations for a New Millennium, pp. 461–487. Ed. by F. Funk, J. Blackburn, D. Hay, A. J. Paul, R. Stephenson, R. Toresen, and D. Witherell. Alaska Sea Grant Publications, Anchorage, AK. 800 pp.

Partridge, B. L., Pitcher, T. J., Cullen, J. M., and Wilson, J. 1980. The three-dimensional structure of fish schools. Behavioral Ecology and Sociobiology, 6: 277–288.

Ranta, E., and Lindström, K. 1990. Assortative schooling in three-spined sticklebacks? Annuales Zoologici Fennici, 27: 67–75.

Ranta, E., Lindström, K., and Peuhkuri, N. 1992. Size matters when three-spined sticklebacks go to school. Animal Behaviour, 43: 160–162.

Sawada, K., Ye, Z., Kieser, R., McFarlane, G. A., Miyanohana, Y., and Furusawa, M. 1999. Target-strength measurements and modelling of walleye pollock and Pacific hake. Fisheries Science, 65: 193–205.

Soule, M. A., Barange, M., and Hampton, I. 1995. Evidence of bias in estimates of target strength obtained with a split-beam echo-sounder. ICES Journal of Marine Science, 52: 139–144.

Soule, M. A., Hampton, I., and Barange, M. 1996. Potential improvements to current methods of recognizing single targets with a split-beam echo-sounder. ICES Journal of Marine Science, 53: 237–243.

Stanton, T. K., Chu, D., and Wiebe, P. H. 1996. Acoustic-scattering characteristics of several zooplankton groups. ICES Journal of marine Science, 53: 289–295.

Tang, M., and Boisclair, D. 1993. Influence of the size of enclosures on the swimming characteristics of juvenile brook trout (*Salvelinus fontinalis*). Canadian Journal of Fisheries and Aquatic Sciences, 50: 1786–1793.

Traynor, J. J. 1996. Target-strength measurements of walleye pollock (*Theragra chalcogramma*) and Pacific whiting (*Merluccius producttus*). ICES Journal of Marine Science, 53: 253–258.

Traynor, J. J., and Ehrenberg, J. E. 1990. Fish and standard-sphere target-strength measurements obtained with a dual-beam and split-beam echo-sounding system. Rapports et Procès-Verbaux des Réunions du Conseil International pourl' Exploration de la Mer, 189: 325–335.

Traynor, J. J., and Williamson, N. J. 1983. Target-strength measurements of walleye pollock (*Theragra chalcogramma*) and a simulation study of the dual-beam method. FAO Fisheries Report, 300: 112–124.

Williamson, N. J., and Traynor, J. J. 1984. *In situ* target-strength estimation of Pacific whiting (*Merluccius productus)* using a duel-beam transducer. Journal du Conseil International pour l'Exploration de la Mer, 41: 285–292.

Ye, Z. 1997. A novel approach to sound scattering by cylinders of finite length. Journal of the Acoustical Society of America, 102: 877–884.

Ye, Z., and Furusawa, M. 1995. Modelling of target strength of swimbladder fish at high frequency. Journal of the Acoustical Society of Japan, 16: 371–379.

Ye, Z., Hoskinson, E., Dewey, R. K., Ding, L., and Farmer, D. M. 1997. A method for acoustic scattering by slender bodies. I. Theory and verification. Journal of the Acoustical Society of America, 102: 1964–1976.

Zhao, X. 1996. Target strength of herring (*Clupea harengus* L.) measured by the split-beam tracking method. Mphil thesis, Department of Fisheries and Marine Biology, Bergen University. 103 pp.